

Rényi entanglement entropy after a quantum quench starting from insulating states in a free boson system

Daichi Kagamihara,^{1,2,*} Ryui Kaneko,^{1,†} Shion Yamashika,² Kota Sugiyama,² Ryosuke Yoshii,³ Shunji Tsuchiya,² and Ippei Danshita¹

¹*Department of Physics, Kindai University, Higashi-Osaka, Osaka 577-8502, Japan*

²*Department of Physics, Chuo University, Tokyo 1-13-27, Japan*

³*Center for Liberal Arts and Sciences, Sanyo-Onoda City University, Yamaguchi 756-0884, Japan*

(Dated: July 19, 2022)

We investigate the time-dependent Rényi entanglement entropy after a quantum quench starting from the Mott-insulating and charge-density-wave states in a one-dimensional free boson system. The second Rényi entanglement entropy is found to be the negative of the logarithm of the permanent of a matrix consisting of time-dependent single-particle correlation functions. From this relation and a permanent inequality, we obtain rigorous conditions for satisfying the volume-law entanglement growth. We also succeed in calculating the time evolution of the entanglement entropy in unprecedentedly large systems by brute-force computations of the permanent. We discuss possible applications of our findings to the real-time dynamics of noninteracting bosonic systems.

I. INTRODUCTION

The concept of entanglement is indispensable for understanding quantum many-body physics these days. A pure quantum many-body state is entangled when it cannot be represented by a product state [1]. The entanglement entropy quantifies the degree of entanglement and is a valuable probe for characterizing states of quantum many-body systems. For example, in critical systems, the entanglement entropy exhibits the universal scaling with the size of a subsystem; the universal coefficient is determined by the corresponding conformal field theory [2–7]. Topologically ordered states, which cannot be described by conventional order parameters, would be characterized by the topological entanglement entropy [8–11].

The von Neumann entanglement entropy is a standard reference value to quantify the entanglement. When a system possesses a pure state $|\psi\rangle$ and can be divided into two subsystems A and B, the entanglement entropy is defined as $S_{\text{vN}} = -\text{Tr} \rho_A \ln \rho_A$, where $\rho_A = \text{Tr}_B \rho$ is the reduced density matrix of $\rho = |\psi\rangle\langle\psi|$. The Rényi entanglement entropy is another quantity, which behaves similarly to the von Neumann entanglement entropy [12, 13], and is defined as $S_\alpha = [\ln \text{Tr}(\rho_A^\alpha)]/(1 - \alpha)$. The von Neumann entanglement entropy can be regarded as the $\alpha \rightarrow 1$ limit of the Rényi entanglement entropy.

The entanglement entropy is not merely an ideal quantity in theory, but it is also measurable experimentally. The protocol for measuring the Rényi entanglement entropy was first proposed in 2012 [13, 14]. In Ref. [13], the authors considered the real-time dynamics of cold atoms in optical lattices, which can be realized in experiments [15], and suggested preparing two copies of the

same state. The Rényi entanglement entropy can be evaluated by controlling the tunnel coupling between these copies and by measuring the parity of the atom numbers. The second Rényi entanglement entropy has been indeed observed during a quench dynamics of one-dimensional (1D) cold atomic gases in an optical lattice [16, 17].

Previous theoretical studies have actively discussed the dynamics of entanglement entropy after a quantum quench in connection with information propagation and thermalization [6, 7, 18–30]. While the dynamics of entanglement entropy in 1D lattice systems can be accurately analyzed by means of numerical methods based on matrix product states [20–25], the tractable time scale is rather limited in general due to the linear growth of the entanglement entropy in time [18]. In the case of 1D fermionic systems, when the system is quenched to a noninteracting parameter region, long-time dynamics can be investigated analytically [18, 29, 31, 32]. In particular, when the initial state is a Gaussian state, i.e., a ground or thermal state of any free (quadratic) Hamiltonian, the time-evolved state remains Gaussian. Then, the time evolution of the entanglement entropy can be evaluated from single-particle correlation functions. The fermionic Gaussian states include simple product states such as the Mott-insulating (MI) and charge-density-wave (CDW) states, which can also be prepared in experiments.

By contrast, studies of the entanglement growth during the quench dynamics for (soft-core) bosons are very few even in the case that the system is quenched to the noninteracting point. This is partly because a simple product state, which is often used as an initial state of quench dynamics in experiments [16, 17], is not a Gaussian state for bosonic systems. Starting from product states such as the MI and CDW states, single-particle correlation functions are analytically calculable [33–35]. However, it is not straightforward to calculate the entanglement entropy from these correlation functions because a time-evolved state is not the Gaussian state.

This situation raises the following questions: (i) Can

* kagamihara@phys.kindai.ac.jp; These two authors contributed equally to this work.

† rkaneko@phys.kindai.ac.jp; These two authors contributed equally to this work.

we get an analytical form of the Rényi entanglement entropy concerning real-time dynamics of noninteracting bosonic systems? (ii) Suppose we obtain the analytical form, can we rigorously obtain conditions under which the volume-law scaling is satisfied during the real-time evolution? (iii) Can we numerically evaluate the Rényi entanglement entropy in systems much larger than the best currently available methods can handle?

To answer these questions, we take the 1D soft-core Bose-Hubbard model as the simplest playground. When the system is quenched to the noninteracting Hamiltonian, we obtain the analytical form of evaluating the second Rényi entanglement entropy. It can be expressed by the expectation value of the shift (swap) operator [13, 14, 16, 17] and is given as the negative of the logarithm of the permanent of a time-dependent matrix consisting of single-particle correlations. We also give the condition for the volume-law scaling of the Rényi entanglement entropy by using a permanent inequality [36]. In addition, we obtain the long-time evolution of the Rényi entanglement entropy in unprecedentedly large systems by numerically computing the matrix permanent. Although direct calculations of the permanent require exponential-time cost in general, accessible sizes are found to be much larger than the exact diagonalization and matrix-product-state methods can deal with. Last but not least, we propose that the infinity norm of rows of the correlation matrix offers an entropy-density-like value and would give a practical bound for the Rényi entanglement entropy. This value would free us from exponential-time computations of the permanent, as long as we are interested in a qualitative behavior of the entanglement entropy growth rather than the value itself.

This paper is organized as follows: In Sec. II, we present the 1D Bose-Hubbard model and introduce two initial states for the quench dynamics. In Sec. III, we calculate the time-evolved states after the sudden quench and derive the analytical form of the Rényi entanglement entropy. In Sec. IV, we summarize some interesting properties of the correlation matrix introduced in Sec. III and show the condition for the volume-law scaling of the Rényi entanglement entropy. In Sec. V, we directly compute the permanent of the correlation matrix and obtain the time evolution of the Rényi entanglement entropy. We also compare our results with other reference values. In addition, we introduce an entropy-density-like value, which can be calculated in polynomial time, and discuss a bound for the Rényi entanglement entropy. In Sec. VI, we draw our conclusions and discuss possible applications to several problems on real-time dynamics of free boson systems. Throughout this paper, we set $\hbar = 1$, take the lattice constant to be unity, and consider the zero-temperature dynamics, for simplicity.

II. 1D BOSE-HUBBARD MODEL

We consider the quench dynamics in the 1D Bose-Hubbard model under the open boundary condition. The Hamiltonian is defined as

$$\hat{H} = -J \sum_{i=1}^{L-1} (\hat{b}_i^\dagger \hat{b}_{i+1} + \text{h.c.}) + \sum_{i=1}^L \Omega_i \hat{n}_i + \frac{U}{2} \sum_{i=1}^L \hat{n}_i (\hat{n}_i - 1). \quad (1)$$

Here the symbols \hat{b}_i and \hat{n}_i denote the boson annihilation and number operators, respectively. The strength of the hopping and the interaction are given as J and U , respectively, and Ω_i denotes the single-particle potential. The length of the chain is represented as L . This model quantitatively describes 1D Bose gases in optical lattices when the lattice potential is sufficiently deep.

We focus on the quench from insulating states to the noninteracting ($U = 0$) and homogeneous ($\Omega_i = 0$) point. As initial states, we specifically choose the MI state at unit filling, which is represented as

$$|\psi^{\text{MI}}\rangle = \prod_{i=1}^L \hat{b}_i^\dagger |0\rangle, \quad (2)$$

and the 010101... CDW state at half filling, which is described as

$$|\psi^{\text{CDW}}\rangle = \prod_{i=2,4,\dots}^L \hat{b}_i^\dagger |0\rangle, \quad (3)$$

where $|0\rangle$ is the vacuum state of \hat{b}_i and L is an even number. The MI state is the ground state of the Bose-Hubbard model at unit filling for large U limit and can be prepared in experiments via a slow ramp-up of the optical lattice potential [16, 17, 35, 37]. The CDW state is the ground state of the Bose-Hubbard model at half filling when $\Omega_i = \Omega(-1)^{i+1}$ and $\Omega/J \gg 1$. It can be prepared in experiments with use of a secondary optical lattice whose lattice constant is twice as large as that of the primary lattice [38].

III. EVALUATING THE SECOND RÉNYI ENTANGLEMENT ENTROPY USING SHIFT OPERATORS

We first consider the time evolution of the many-body wave function. Since the matrix representation of the single-particle Hamiltonian after the quench is tridiagonal, we easily find the single-particle energy

$$\epsilon_k = -2J \cos\left(\frac{k\pi}{L+1}\right) \quad (4)$$

and corresponding eigenstate

$$x_{kl} = \sqrt{\frac{2}{L+1}} \sin\left(\frac{k\pi}{L+1}l\right), \quad (5)$$

where $k, l = 1, 2, \dots, L$. The time-evolved many-body states $|\psi(t)\rangle = e^{-i\hat{H}t}|\psi(0)\rangle$ are given as

$$|\psi^{\text{MI}}(t)\rangle = \prod_{i=1}^L \left[\sum_{j=1}^L y_{ij}(t) \hat{b}_j^\dagger \right] |0\rangle, \quad (6)$$

$$|\psi^{\text{CDW}}(t)\rangle = \prod_{i=2,4,\dots}^L \left[\sum_{j=1}^L y_{ij}(t) \hat{b}_j^\dagger \right] |0\rangle, \quad (7)$$

where all information about real-time dynamics is encoded in

$$y_{ij}(t) = \sum_{k=1}^L x_{ki} e^{-i\epsilon_k t} x_{kj}. \quad (8)$$

The second Rényi entanglement entropy can be obtained by utilizing the expectation value of the shift (swap) operator \hat{V} [13, 14, 16, 17]. Let us suppose that we have two copies of the state $|\psi(t)\rangle$, which we call copies 1 and 2, and that the total wave function is given by the product state of the two copies,

$$|\psi_{\text{copy}}(t)\rangle = |\psi(t)\rangle \otimes |\psi(t)\rangle. \quad (9)$$

We divide the system into two subsystems A and B. Here the subsystem A contains $j = 1, 2, \dots, L_A$ sites in this paper. Let us consider the shift operator \hat{V}_B which swaps states in the subsystem B. The expectation value of \hat{V}_B in terms of $|\psi_{\text{copy}}(t)\rangle$ is related to the reduced density matrix $\hat{\rho}_A$ as

$$\langle \psi_{\text{copy}}(t) | \hat{V}_B | \psi_{\text{copy}}(t) \rangle = \text{Tr} \hat{\rho}_A^2. \quad (10)$$

As long as \hat{V}_B acts on a product state of copies 1 and 2, such as Eq. (9), the shift operator transforms the creation operator as

$$\hat{V}_B \hat{b}_j^\dagger \hat{V}_B^{-1} = \begin{cases} \hat{b}_j^\dagger & (j \in \text{A}) \\ \hat{c}_j^\dagger & (j \in \text{B}) \end{cases}, \quad (11)$$

$$\hat{V}_B \hat{c}_j^\dagger \hat{V}_B^{-1} = \begin{cases} \hat{c}_j^\dagger & (j \in \text{A}) \\ \hat{b}_j^\dagger & (j \in \text{B}) \end{cases}, \quad (12)$$

where operators \hat{b} and \hat{c} respectively correspond to boson operators for the copies 1 and 2. For derivation of Eqs. (11) and (12), see Appendix A. Making use of these relations, we can evaluate the second Rényi entanglement entropy in an elementary way. For example, for the MI state, it can be evaluated as

$$S_2 = -\ln \langle \psi_{\text{copy}}^{\text{MI}}(t) | \hat{V}_B | \psi_{\text{copy}}^{\text{MI}}(t) \rangle, \quad (13)$$

$$|\psi_{\text{copy}}^{\text{MI}}(t)\rangle = \left\{ \prod_{i=1}^L \left[\sum_{j=1}^L y_{ij}(t) \hat{b}_j^\dagger \right] \right\} \cdot \left\{ \prod_{i=1}^L \left[\sum_{j=1}^L y_{ij}(t) \hat{c}_j^\dagger \right] \right\} |0\rangle^{\otimes 2}, \quad (14)$$

$$\hat{V}_B |\psi_{\text{copy}}^{\text{MI}}(t)\rangle = \left\{ \prod_{i=1}^L \left[\sum_{j=1}^{L_A} y_{ij}(t) \hat{b}_j^\dagger + \sum_{j=L_A+1}^L y_{ij}(t) \hat{c}_j^\dagger \right] \right\} \cdot \left\{ \prod_{i=1}^L \left[\sum_{j=1}^{L_A} y_{ij}(t) \hat{c}_j^\dagger + \sum_{j=L_A+1}^L y_{ij}(t) \hat{b}_j^\dagger \right] \right\} |0\rangle^{\otimes 2}. \quad (15)$$

Since both $|\psi_{\text{copy}}^{\text{MI}}(t)\rangle$ and $\hat{V}_B |\psi_{\text{copy}}^{\text{MI}}(t)\rangle$ are many-boson states, the expectation value $\langle \psi_{\text{copy}}(t) | \hat{V}_B | \psi_{\text{copy}}(t) \rangle$ can be rewritten by the permanent of the Hermitian matrix A :

$$S_2 = -\ln \text{perm} A, \quad (16)$$

$$A = \begin{pmatrix} Z & I - Z \\ I - Z & Z \end{pmatrix}. \quad (17)$$

Here I is an identity matrix and Z is a single-particle overlap matrix between single-particle states $e^{-i\hat{H}t} \hat{b}_i^\dagger |0\rangle$ and $\hat{V}_B e^{-i\hat{H}t} \hat{b}_j^\dagger |0\rangle$. The element z_{ij} of the Hermitian matrix Z is given as

$$z_{ij}^{\text{MI}} = \sum_{l=1}^{L_A} y_{il}^*(t) y_{jl}(t) \quad (i, j = 1, 2, \dots, L), \quad (18)$$

$$z_{ij}^{\text{CDW}} = \sum_{l=1}^{L_A} y_{il}^*(t) y_{jl}(t) \quad (i, j = 2, 4, \dots, L). \quad (19)$$

Note that a somewhat similar formula for the Rényi entanglement entropy given by the permanent has been proposed for excited states in the static system [39].

In the following, \tilde{L} denotes the size of the square matrix A . It is given by $2\nu L$, where ν is the filling fraction. For example, $\tilde{L} = 2L$ (L) for the MI (CDW) state. Hereafter we will mainly consider the entanglement entropy for a bipartition of the system into two half-chains ($L_A = L/2$).

IV. ANALYTICAL RESULTS

In this section, we analytically evaluate the size L dependence of the Rényi entanglement entropy S_2 by examining the permanent of the matrix A . We will discuss the condition for S_2 to satisfy the volume-law scaling.

A. Remarks on the matrices Z and A

Let us first summarize the characteristics of the matrices Z and A . The purpose of this subsection is to show $\|A\|_2 = 1$ for both MI and CDW initial states. Here the operator 2-norm is defined as $\|A\|_2 := \sup_{\|\mathbf{x}\|_2 \leq 1, \mathbf{x} \in \mathbb{C}^{\tilde{L}}} \|A\mathbf{x}\|_2$ [on the right hand side of the equation, $\|\mathbf{x}\|_p := (\sum_i |x_i|^p)^{1/p}$ is an L^p norm of a vector \mathbf{x}], or the largest singular value of the matrix A . We will

utilize this fact to obtain the condition for the volume-law entanglement growth in the next subsection.

For the quench from the MI state, the matrix Z^{MI} is a complex orthogonal projection matrix, satisfying $(Z^{\text{MI}})^2 = Z^{\text{MI}} = (Z^{\text{MI}})^\dagger$ (see Appendix B). Therefore, all the eigenvalues are either 0 or 1. For the quench from the CDW state, the matrix Z^{CDW} is a principal submatrix of the Hermitian matrix Z^{MI} , i.e., it can be obtained from Z^{MI} by removing L rows and the same L columns. Using the Cauchy's interlace theorem [40, 41], we can show that all the eigenvalues of Z^{CDW} are bounded by the largest eigenvalue 1 and the smallest eigenvalue 0 of Z^{MI} . As a result, $0 \leq \|Z^{\text{CDW}}\|_2 \leq \|Z^{\text{MI}}\|_2 \leq 1$.

All the eigenvalues of the matrix A can be obtained from those of Z . Let us write the eigenvalues of Z as $\epsilon_i^{(Z)}$ and the eigenvectors of Z as $|\epsilon_i^{(Z)}\rangle = (v_{i1}, v_{i2}, \dots, v_{in})^T$ for $i = 1, 2, \dots, n$ with n being the length of the square matrix Z . Then, half of all the eigenvalues of A are $\epsilon_i^{(A)} = 1$, and the corresponding eigenvectors are $|\epsilon_i^{(A)}\rangle = (v_{i1}, v_{i2}, \dots, v_{in}, v_{i1}, v_{i2}, \dots, v_{in})^T$. The remaining half are $\epsilon_i^{(A)} = 2\epsilon_i^{(Z)} - 1$, and the corresponding eigenvectors are $|\epsilon_i^{(A)}\rangle = (v_{i1}, v_{i2}, \dots, v_{in}, -v_{i1}, -v_{i2}, \dots, -v_{in})^T$. Therefore, $\epsilon_i^{(A)} \in [-1, 1]$ because $\epsilon_i^{(Z)} \in [0, 1]$, and, in particular, $\max \epsilon_i^{(A)} = 1$. Thus, the operator 2-norm of the matrix A satisfies $\|A\|_2 = 1$.

For the quench from the MI state, the matrix A^{MI} becomes a unitary matrix, which can be shown by the relations $(Z^{\text{MI}})^2 + (I - Z^{\text{MI}})^2 = Z^{\text{MI}} + (I - Z^{\text{MI}}) = I$ and $Z^{\text{MI}}(I - Z^{\text{MI}}) = 0$. This unitarity also ensures $\|A\|_2 = 1$. For the quench from the CDW state, the matrix A is not a unitary matrix in general; however, $\|A\|_2 = 1$ still holds.

Note that the elements of matrix A satisfy

$$\sum_j a_{ij} = 1, \quad \sum_i a_{ij} = 1 \quad (20)$$

for any rows i and columns j , which is a part of the definition of the doubly stochastic matrix while the positivity condition $a_{ij} > 0$ is absent. (Here the matrix A is complex and satisfies $0 \leq |a_{ij}| \leq 1$.) The permanent of the doubly stochastic matrix has been intensively studied [42–49], while little is known about the permanent of a general complex matrix so far.

B. Condition for volume-law entanglement entropy

To quantify the \tilde{L} dependence of the entanglement entropy, we utilize the inequality [36]

$$|\text{perm}A| \leq C^{\tilde{L}} \exp \left\{ -10^{-5} \times \left[1 - \frac{g(\tilde{L})}{C} \right]^2 \tilde{L} \right\}, \quad (21)$$

which holds for an arbitrary $\tilde{L} \times \tilde{L}$ complex matrix A and an arbitrary nonzero constant C satisfying $C \geq \|A\|_2$. The function $g(\tilde{L})$ is defined as $g(\tilde{L}) := \sum_i \|\mathbf{r}_i\|_\infty / \tilde{L}$ with

\mathbf{r}_i 's being rows of a matrix A and $\|\mathbf{x}\|_\infty := \max_i |x_i|$, which satisfies $0 \leq g(\tilde{L}) \leq \|A\|_2$. In the present case, from Eq. (10), $\text{perm}A$ equals $\text{Tr} \rho_A^2$, implying $\text{perm}A > 0$. In addition, because $\|A\|_2 = 1$, we can choose $C = 1$ as the tightest bound. Then, the inequality is simplified as

$$\text{perm}A \leq \exp \left\{ -10^{-5} \times \left[1 - g(\tilde{L}) \right]^2 \tilde{L} \right\}. \quad (22)$$

Note that $|\text{perm}A| \leq 1$ holds for any unitary matrix A [50], as is the case with the quench from the MI state. Even if A is nonunitary, as is the case with the quench from the CDW state, $|\text{perm}A| \leq (\|A\|_2)^{\tilde{L}}$ holds [51]. Equation (21) gives a much tighter constraint on the permanent of A than these two inequalities.

Consequently, the Rényi entanglement entropy satisfies

$$S_2 \geq 10^{-5} \times \left[1 - g(\tilde{L}) \right]^2 \tilde{L}. \quad (23)$$

This inequality rigorously guarantees that when

$$\lim_{\tilde{L} \rightarrow \infty} \left[1 - g(\tilde{L}) \right] \neq 0, \quad (24)$$

the Rényi entanglement entropy shows the volume-law scaling. In other words, when Eq. (24) holds, the area-law scaling (and the area-law scaling with a logarithmic correction, as is often the case in critical systems [2–5]) is prohibited. We note that if $\lim_{\tilde{L} \rightarrow \infty} [1 - g(\tilde{L})] = 0$, Eq. (23) becomes meaningless and either the area-law or volume-law scaling is allowed. From the volume-law condition given in Eq. (24), we expect that the value $1 - g(\tilde{L})$ (≥ 0) could be used as an entropy-density-like value, which we will discuss in Sec. V E.

V. NUMERICAL RESULTS

In this section, we will numerically evaluate the permanent to obtain the Rényi entanglement entropy. In general, permanent calculations require an exponentially long time. However, we can practically obtain the Rényi entanglement entropy for systems larger than the exact diagonalization method can handle and can perform longer simulations than the method based on matrix product states, even by performing a brute-force permanent calculation.

The advantages of getting the Rényi entanglement entropy by the permanent calculation are the followings: (i) We do not need Hamiltonian eigenstates, which require much memory cost. This is the main reason why our method enables us to access larger systems than the exact diagonalization method can handle. (ii) Without explicit time evolution, we can directly calculate the Rényi entanglement entropy at a given time, which allows us parallel computations. (iii) In a system of soft-core bosons, there is no upper limit to the number of bosons at any site, but it is common to set the realistic limit when performing numerical calculations. With the present method we

have proposed, we do not have to care about the size of such a local Hilbert space.

A. Summary of algorithm

Here we briefly review the algorithm for the permanent calculation.

The permanent of an $n \times n$ matrix A is defined as

$$\text{perm}A = \sum_{\sigma \in \text{Sym}(n)} \prod_{i=1}^n a_{i,\sigma(i)}, \quad (25)$$

where $\text{Sym}(n)$ is the symmetric group, i.e., over all permutations of numbers $1, 2, \dots, n$. Since straightforward calculations require $n! \times n$ arithmetic operations, we should use a more efficient algorithm. The best known algorithms so far are the Ryser formula [52–54] and Balasubramanian-Bax-Franklin-Glynn (BBFG) formula [54–58]. Both take $\mathcal{O}(n2^{n-1})$ computation time. Hereafter we mainly use the BBFG formula for the permanent calculation. It is given by

$$\text{perm}A = \frac{1}{2^{n-1}} \sum_{\delta} \left(\prod_{k=1}^n \delta_k \right) \prod_{j=1}^n \sum_{i=1}^n \delta_i a_{ij}, \quad (26)$$

where $\delta = (\delta_1, \delta_2, \dots, \delta_n) \in \{\pm 1\}^n$ with $\delta_1 = 1$. Although the computation time using the above straightforward BBFG formula is $\mathcal{O}(n2^{2n-1})$, it can be reduced to $\mathcal{O}(n2^{n-1})$ by utilizing a specific ordering of the binary numeral system, known as Gray code [59, 60]. Our numerical source code is based on the python program in “The Walrus” library [61].

The current feasible matrix size is up to $\sim 50 \times 50$ [62–64]. For a quench from the MI (CDW) state, the size of the matrix A is $2L \times 2L$ ($L \times L$). Therefore, in principle, we may handle $L \lesssim 25$ ($L \lesssim 50$) for the MI (CDW) case. Here we present our results for $L \leq 20$ ($L \leq 40$) for the quench from the MI (CDW) state. Although we may be able to utilize the symmetry of the matrix A to accelerate permanent computations [65], we stick to the original BBFG formula. Even without improving the original algorithm, it allows us to calculate the permanent for systems much larger than the exact diagonalization method can deal with. (Note that, for example, exact diagonalization calculations for $L = 14$ from the MI state to $U/J = 3.01$ have been reported [23].) As for the size at which the permanent is computable, the entanglement can be obtained at any given time, allowing for longer simulations than the methods based on matrix product states.

B. Time dependence of entanglement entropy

We examine the time dependence of the Rényi entanglement entropy (see Fig. 1). For a short time ($tJ \lesssim$

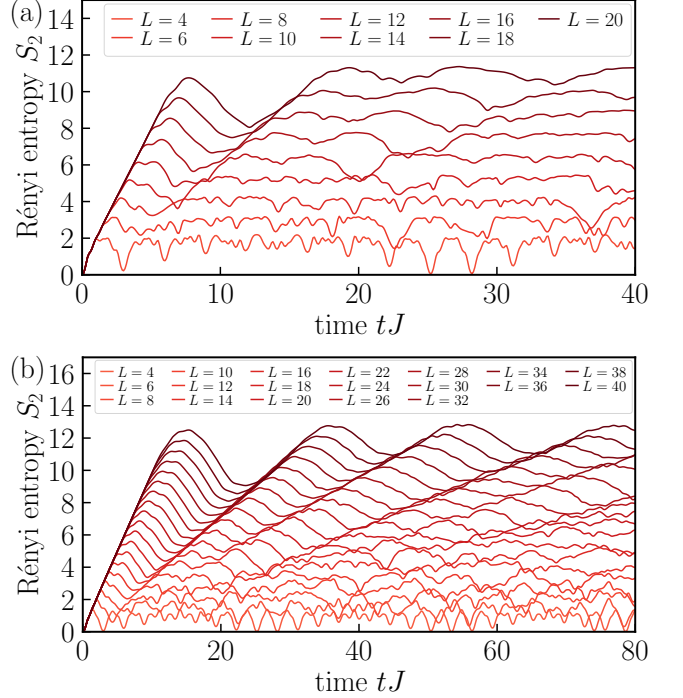


FIG. 1. Time dependence of the Rényi entanglement entropy for (a) the MI and (b) CDW states. For a short time ($tJ \lesssim L/4$), the Rényi entanglement entropy S_2 exhibits an increase proportional to time t . After a long time ($tJ \gtrsim L/4$), S_2 is nearly saturated at the value proportional to the system size L .

$L/4$), S_2 grows linearly with t . After $tJ \gtrsim L/4$, S_2 is almost saturated and reaches the value nearly proportional to L . S_2 exhibits oscillations whose period grows with L . These observations are consistent with the fact that the t -linear growth of entanglement terminates at $t \sim L/(2v)$, where v is the maximum quasiparticle velocity [27]. The velocity is given by the width of dispersion (when $\hbar = 1$ and the lattice constant is chosen to be unity) and, in the present 1D free boson system, $v = 2J$ [34, 35].

To see this behavior more clearly, we rescale the time tJ and the entanglement entropy S_2 in the unit of the system size L (see Fig. 2). All the lines are nearly overlap for $tJ/L \lesssim 1$ when $L \gtrsim 10$ ($L \gtrsim 20$) for the quench from the MI (CDW) state. The deviation from the thermodynamic limit appears to be smaller for the CDW state because the feasible size is larger than the MI state.

C. Comparison with the Rényi entanglement entropy estimated from the Gaussian state

Although the integrable system does not thermalize, the MI or CDW state quenched to $U = 0$ evolves to a Gaussian state after a long time in the thermodynamic limit ($L \gg tJ \gg 1$) [33, 66, 67]. The entanglement entropy of the Gaussian state can be calculated from the eigenvalues of the correlation matrix, consisting of

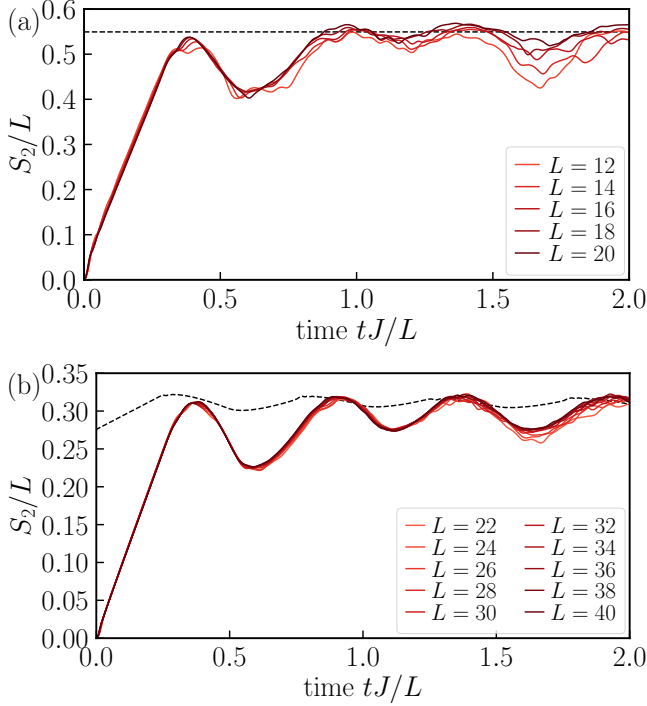


FIG. 2. Rescaled time dependence of the Rényi entanglement entropy for (a) the MI and (b) CDW states. The entanglement entropy and the time are rescaled by L . The dashed lines correspond to the Rényi entanglement entropy densities S_2^{Gaussian}/L estimated from Eq. (27). The dashed line is independent of L for the MI state, while it is obtained for a sufficiently large size ($L = 256$) for the CDW state.

$\langle b_i^\dagger b_j \rangle$ and $\langle b_i b_j \rangle$ [18, 29, 31, 32, 68]. After diagonalizing the correlation matrix in bosonic systems, we obtain the eigenvalues, which correspond to the expectation values of the mode occupation numbers n_k . The Rényi entanglement entropy S_α of order α can be described by n_k as [18, 29, 31, 32, 68]

$$S_\alpha = \frac{1}{\alpha - 1} \sum_k \ln [(n_k + 1)^\alpha - n_k^\alpha]. \quad (27)$$

The time-evolved state is not a Gaussian state for $tJ, L < \infty$ in general. However, it is not outrageous to extract reference values using the Gaussian state, which exhibits the same single-particle correlation functions of the (non-Gaussian) time-evolved state for a finite time and finite sizes. At least for the MI quench, as we see below, single-particle correlations are independent of time and size. As a result, the Rényi entanglement entropy of Eq. (27) obtained from the mode occupation numbers n_k for any $tJ, L < \infty$ gives the true Rényi entanglement entropy for $tJ, L \gg 1$. Hereafter we use the symbol S_2^{Gaussian} to denote the Rényi entanglement entropy estimated from Eq. (27).

For the quench starting from the MI state, the correlation matrix is already diagonal; $\langle b_i^\dagger b_j \rangle = \delta_{ij}$ and $\langle b_i b_j \rangle = 0$ for all L and tJ . The mode occupation numbers, $n_k = 1$

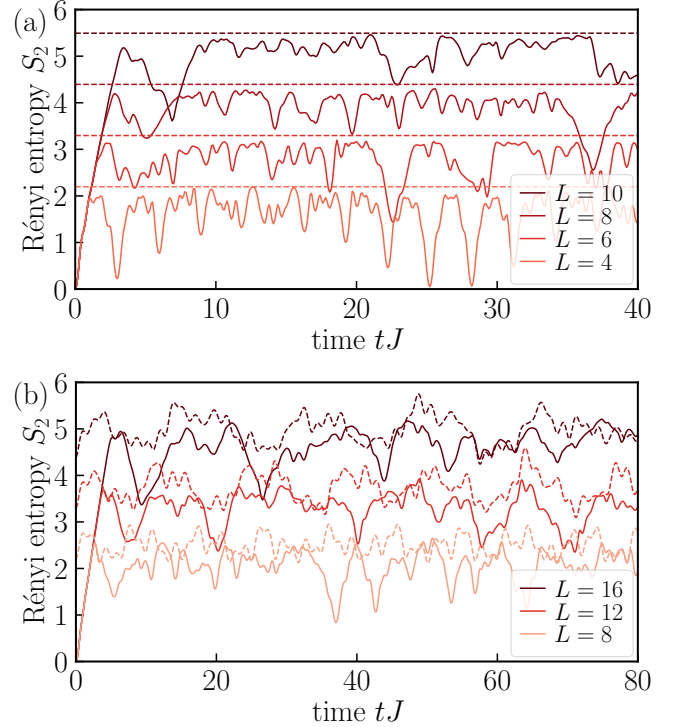


FIG. 3. Comparisons between the Rényi entanglement entropy S_2 (solid lines) and that estimated from Eq. (27) S_2^{Gaussian} (dashed lines) for (a) the MI and (b) CDW states.

($k = 1, 2, \dots, L_A$), are independent of time and sizes. Therefore, the Rényi entanglement entropy for a subsystem $L_A = L/2$ is $S_2^{\text{Gaussian}} = \ln 3 \times L/2 \sim 0.5493 \times L$. Indeed, numerically obtained S_2 for $tJ \gg L$ fluctuates around S_2^{Gaussian} [see Fig. 2(a) and Fig. 3(a)], while a t -linear growth is not reproduced in S_2^{Gaussian} for a short time ($tJ \ll L$).

For the quench starting from the CDW state, we numerically evaluate the Rényi entanglement entropy for a subsystem $L_A = L/2$. In this case, $\langle b_i^\dagger b_j \rangle$ depends on time, and therefore, S_2^{Gaussian} oscillates in time. Again, numerically obtained S_2 for $tJ \gg L$ fluctuates around S_2^{Gaussian} [see Fig. 2(b) and Fig. 3(b)], whereas a t -linear growth in a short time is absent for S_2^{Gaussian} . The Rényi entanglement entropy in the thermodynamics limit for a long time is estimated to be $S_2^{\text{Gaussian}}/L = 0.31(1)$ for the Gaussian state, and S_2 is expected to converge to this value for $tJ, L \gg 1$.

D. Comparison with Page value

The system is thermalized when it is quenched to the parameter region $|U| > 0$ [69, 70]. The entanglement entropy would nearly saturate at the entanglement of the random state vector, which is known as the Page value [71]. For the Bose-Hubbard model, an analytical expression for the Page value has not been obtained yet.

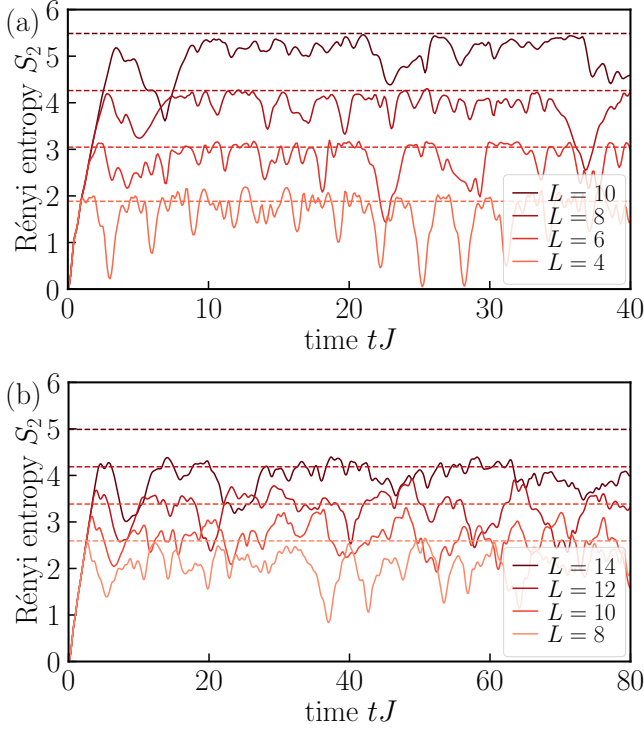


FIG. 4. Comparisons between the calculated Rényi entanglement entropy (solid lines) and the Page value (dashed lines) for (a) the MI and (b) CDW states.

We can obtain the Page value within the statistical error bars by numerically taking an average of random state vectors [25, 72].

When $U = 0$, the time-evolved state is not thermalized. The Rényi entanglement entropy, in this case, would deviate from the Page value. To examine whether we can tell the difference between the entanglement entropy of the thermalized state and that of the state quenched to $U = 0$, we compare the Rényi entanglement entropy at $U = 0$ with the Page value. We calculate the Page value by averaging 1024 random samples.

As for the quench from the MI state, the Page value S_2^{Page} at unit filling $\nu = 1$ is close to the Rényi entanglement entropy S_2 for a longer time ($tJ \gtrsim L/4$) and for all systems ($L \leq 10$) that we have considered [see Fig. 4(a)]. This observation suggests that the entropies for $U = 0$ and $|U| > 0$ after the long-time evolution are nearly continuously connected at unit filling. Even though the time-evolved state does not thermalize, we may observe a somewhat similar relaxation process as in the case of $|U| > 0$ unexpectedly.

On the other hand, for the quench from the CDW state at half filling $\nu = 1/2$, the Rényi entanglement entropy S_2 is slightly smaller than the Page value [see Fig. 4(b)]. The deviation seems to be more enhanced with increasing system sizes. It is likely that the Rényi entanglement entropy density would be smaller than the density of the Page value in the thermodynamic limit although the

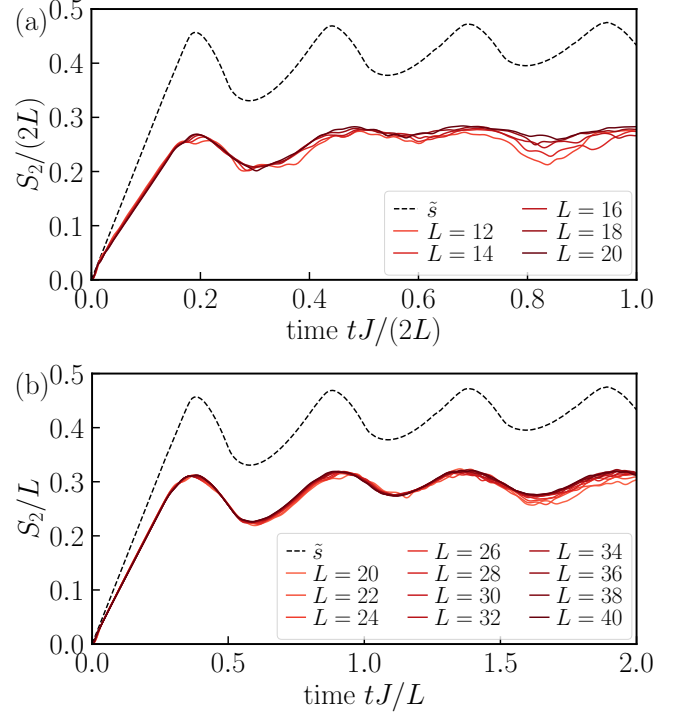


FIG. 5. Comparisons between the rescaled Rényi entanglement entropy S_2/\tilde{L} and $\tilde{s}(\tilde{L})$ estimated from the infinity norm of rows of the matrix A for (a) the MI ($\tilde{L} = 2L$) and (b) CDW ($\tilde{L} = L$) states. The value $\tilde{s}(\tilde{L})$ is obtained for a sufficiently large size ($L = 256$).

Rényi entanglement entropy itself satisfies the volume-law scaling, as can be seen from Fig. 2(b). Unlike the MI case, it is expected that a jump occurs between the entropies of $U = 0$ and $|U| > 0$ quenches after long-time evolution. In this respect, we compare the entanglement entropy of $U = 0$ with that of $U > 0$ and confirm the presence of a jump in Appendix C.

E. Entropy-density-like value and practical bound for the Rényi entanglement entropy

From the argument in Sec. IV B, we obtain the rigorous lower bound for the second Rényi entanglement entropy density, which is given as

$$\frac{S_2}{\tilde{L}} \geq 10^{-5} \times \left[1 - g(\tilde{L})\right]^2. \quad (28)$$

Moreover, the tighter bound was conjectured to be $\text{perm} A \leq e^{-\text{const.} \times \tilde{L}[1-g(\tilde{L})]}$ [36], which gives the lower bound of the entanglement entropy as

$$\frac{S_2}{\tilde{L}} \geq \text{const.} \times \left[1 - g(\tilde{L})\right]. \quad (29)$$

We briefly note that the conjectured bound gives the same condition for the volume-law entanglement growth

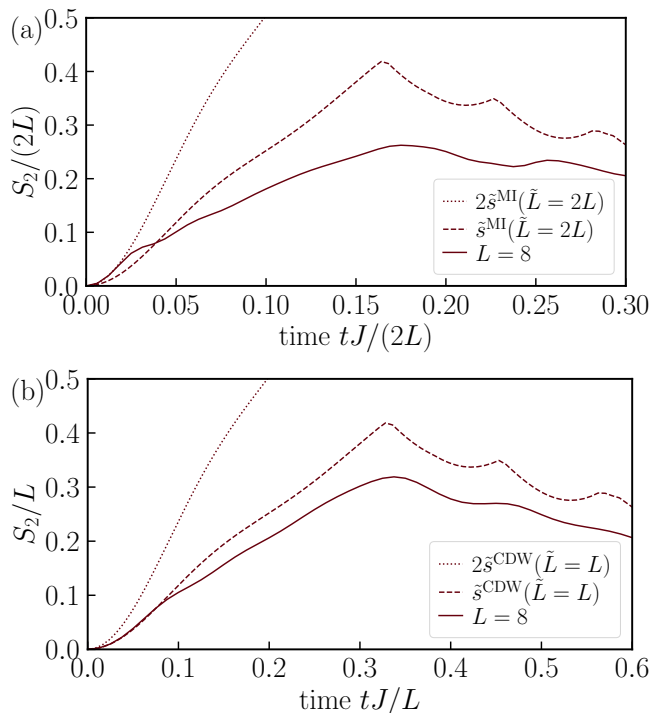


FIG. 6. Comparisons between the rescaled Rényi entanglement entropy S_2/\tilde{L} and $\tilde{s}(\tilde{L})$ estimated from the infinity norm of rows of the matrix A for (a) the MI ($\tilde{L} = 2L$) and (b) CDW ($\tilde{L} = L$) states for $L = 8$. In the both cases, the Rényi entanglement entropy density S_2/L seems to be bounded by $2\tilde{s}(\tilde{L})$. Note that $\tilde{s}(\tilde{L})$'s are the same for the MI and CDW states; however, this is accidental, and we have confirmed that those of CDW states with other periodicities exhibit different behavior (although we do not explicitly show those here).

as Eq. (24). These inequalities lead us to expect that $\tilde{s}(\tilde{L}) = 1 - g(\tilde{L})$ determines qualitative behavior of the Rényi entanglement entropy density and serves as an entropy-density-like value. $\tilde{s}(\tilde{L})$ is obtained from the infinity norm of rows of the matrix A :

$$\tilde{s}(\tilde{L}) = 1 - \frac{1}{\tilde{L}} \sum_i \max_j \{|z_{ij}|, |\delta_{ij} - z_{ij}|\}. \quad (30)$$

Unlike the permanent of a matrix A , which requires costly calculation, $\tilde{s}(\tilde{L})$ is easy to compute numerically and analytically. Hence if $\tilde{s}(\tilde{L})$ has the similar tendency with S_2/\tilde{L} , it would be a helpful quantity to qualitatively capture features of the entropy density.

To see the behavior of $\tilde{s}(\tilde{L})$ in the thermodynamic limit, we compare $\tilde{s}(\tilde{L})$ for a much larger system ($L = 256$) with S_2/\tilde{L} for $\tilde{L} \leq 40$ in Fig. 5. Both $\tilde{s}(\tilde{L})$ and S_2/\tilde{L} are found to behave in the qualitatively similar way including the period of oscillations. Thus, we confirm that $\tilde{s}(\tilde{L})$ certainly captures the qualitative behavior of the Rényi entanglement entropy density.

While Eq. (29) means that $\text{const.} \times \tilde{s}(\tilde{L})$ serves as a lower bound of S_2/\tilde{L} , we observe in Fig. 5 that the

rescaled Rényi entanglement entropy S_2/\tilde{L} would be practically bounded from above by the value $\tilde{s}(\tilde{L})$. This observation motivates us to examine how $\tilde{s}(\tilde{L})$ bounds the entanglement entropy S_2/\tilde{L} from above. For this purpose, we compare these for a given \tilde{L} , as shown in Fig. 6. We find a region where the expected inequality $S_2/\tilde{L} < \tilde{s}(\tilde{L})$ is slightly violated. Even in this case, for the MI quench, S_2/\tilde{L} is bounded by $2\tilde{s}(\tilde{L})$ from above and they well overlap in the time range $tJ/(2L) \lesssim 0.02$ [see Fig. 6(a)]. Likewise, in the case of the CDW quench, $2\tilde{s}(\tilde{L})$ still gives an upper bound for S_2/\tilde{L} [see Fig. 6(b)]. From these observations, we speculate that some constant value times $\tilde{s}(\tilde{L})$ would practically give an upper bound of the Rényi entanglement entropy.

To sum up this subsection, we have observed

$$\frac{S_2}{\tilde{L}} \lesssim \tilde{s}(\tilde{L} \rightarrow \infty) \quad \text{for } \tilde{L} \gg 1, \quad (31)$$

$$\frac{S_2}{\tilde{L}} \lesssim \text{const.} \times \tilde{s}(\tilde{L}) \quad \text{for any finite } \tilde{L}. \quad (32)$$

These results imply that $\tilde{s}(\tilde{L})$, which can be obtained from the infinity norm of rows of the matrix A , would be a helpful guide in estimating the Rényi entanglement entropy at least in the present case. We expect that the current discussion is applicable to other initial conditions and Hamiltonians.

VI. SUMMARY AND OUTLOOK

We have studied the time evolution of the Rényi entanglement entropy in a 1D free boson system. We have focused on the quench dynamics of the 1D Bose-Hubbard model at the noninteracting point starting from the Mott-insulating and charge-density-wave initial states. We have obtained the analytical form of the second Rényi entanglement entropy by calculating the expectation value of the shift operator. The entanglement entropy was found to be the negative of the logarithm of the permanent of the correlation matrix, whose elements are time-dependent single-particle correlation functions. Using a permanent inequality, we have rigorously proven that the Rényi entanglement entropy satisfies the volume-law scaling under a certain condition. We have also numerically obtained the long-time evolution of the Rényi entanglement entropy by direct computations of the permanent. Although it requires exponential time in general, the present approach is superior to the best currently available methods such as the exact diagonalization and matrix-product-state methods. The feasible system size is about twice the size that the conventional method can handle [23].

The procedure presented in this paper can be extended to systems containing long-range hopping parameters and those with randomness. Real-time dynamics of such complex quantum many-body systems of free fermions have attracted much attention recently, whereas those

of free bosons are yet to be explored because of their computational difficulties. Our method would be helpful for studying such bosonic counterparts. Typical examples include (i) noninteracting higher-dimensional systems (see Refs. [73–75] for correlation-spreading dynamics with a quench to $U \ll J$ in 2D), (ii) Anderson localization with long-range hopping (see Refs. [76] and [77] for free fermions), (iii) localization in disorder-free or correlated-disorder systems such as the Aubry-André model [78] (see Refs. [76] and [79] for free fermions), and (iv) Lindblad dynamics of free bosons (see Refs. [80–84] for free fermions).

We have introduced the entropy-density-like value using the infinity norm of rows of the correlation matrix and have numerically demonstrated that it well captures the features of the Rényi entanglement entropy density. We have also discussed a practical bound of the entanglement entropy, i.e., that of the matrix permanent, which usually requires exponential time computations. Our findings on the practical bound would also stimulate mathematical research on the permanent of general complex matrices and research in the field of quantum computing involving boson-sampling techniques [85, 86].

ACKNOWLEDGMENTS

The authors acknowledge fruitful discussions with S. Goto and Y. Takeuchi. This work was financially supported by JSPS KAKENHI (Grants Nos. 18H05228, 19K14616, 20H01838, 21H01014, and 21K13855), by Grant-in-Aid for JSPS Fellows (Grant No. 22J22306), by JST CREST (Grant No. JPMJCR1673), by MEXT Q-LEAP (Grant No. JPMXS0118069021), and by JST FOREST (Grant No. JPMJFR202T).

Appendix A: Derivation of Eqs. (11) and (12)

Although we apply Eqs. (11) and (12) to the product state of the same state living in copies 1 and 2, such as Eq. (9), in the main part, it holds even if states of copies 1 and 2 are different. To prove this, we first Schmidt decompose the state of copies 1(2) as

$$|\psi\rangle^{1(2)} = \sum_l s_l^{1(2)} |\phi_l\rangle^{1(2),A} |\varphi_l\rangle^{1(2),B}, \quad (\text{A1})$$

where $|\phi_l\rangle^{1(2),A}$ and $|\varphi_l\rangle^{1(2),B}$ are orthonormal states of subsystem A and B, respectively. $s_l^{1(2)}$ is the Schmidt coefficient. The product state of copies 1 and 2 is given by

$$|\psi_{\text{prod}}\rangle = |\psi\rangle^1 \otimes |\psi'\rangle^2, \quad (\text{A2})$$

where we assume that copies 1 and 2 can have different states.

We consider how $\hat{V}_B \hat{b}_j^\dagger \hat{V}_B^{-1}$ acts on the state given by Eq. (A2). Note that $\hat{V}_B^{-1} = \hat{V}_B$ holds because of $\hat{V}_B^2 =$

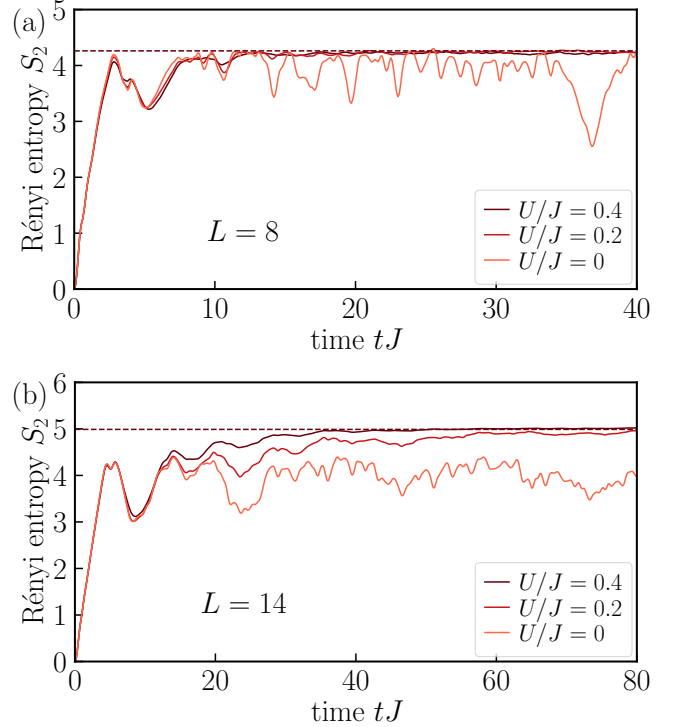


FIG. 7. Comparisons of the time evolution of the Rényi entropies for the quench to $U/J = 0, 0.2$, and 0.4 from (a) the MI and (b) CDW initial states. The dashed line shows the Page value as the expected entanglement entropy when thermalization occurs. For finite U/J , the entanglement entropy is calculated from the exact diagonalization method [87, 88]. To reduce the memory cost, it is calculated from the singular value decomposition of a wave function utilizing $U(1)$ symmetry [89], associated with the conservation of the total particle number [90–93].

\hat{I} . When $j \in A$, $\hat{V}_B \hat{b}_j^\dagger \hat{V}_B^{-1} |\psi_{\text{prod}}\rangle = \hat{b}_j^\dagger |\psi_{\text{prod}}\rangle$ trivially holds. In the case of $j \in B$, the action of $\hat{V}_B \hat{b}_j^\dagger \hat{V}_B^{-1}$ on the product state is given by

$$\begin{aligned} & \hat{V}_B \hat{b}_j^\dagger \hat{V}_B^{-1} |\psi_{\text{prod}}\rangle \\ &= \hat{V}_B \hat{b}_j^\dagger \sum_{l,m} s_l^1 s_m'^2 |\phi_l\rangle^{1,A} |\varphi_m'\rangle^{1,B} |\phi_m'\rangle^{2,A} |\varphi_l\rangle^{2,B} \\ &= \hat{V}_B \sum_{l,m} s_l^1 s_m'^2 |\phi_l\rangle^{1,A} (\hat{b}_j^\dagger |\varphi_m'\rangle^{1,B}) |\phi_m'\rangle^{2,A} |\varphi_l\rangle^{2,B} \\ &= \sum_{l,m} s_l^1 s_m'^2 |\phi_l\rangle^{1,A} |\varphi_l\rangle^{1,B} |\phi_m'\rangle^{2,A} (c_j^\dagger |\varphi_m'\rangle^{2,B}) \\ &= c_j^\dagger |\psi_{\text{prod}}\rangle. \end{aligned} \quad (\text{A3})$$

Thus, we proved Eq. (11) [and Eq. (12) in the same manner] as long as it acts on the product state of copies 1 and 2.

Appendix B: More on the property of the matrix Z^{MI}

The matrix X , having the element x_{kl} in Eq. (5), is unitary and diagonalizes the Hamiltonian H , namely, $HX = XE$, with the matrix E being a diagonal matrix consisting of all the corresponding eigenvalues. The matrix $D = e^{-iEt}$ ($t \geq 0$) is also unitary, and the matrix Y , having the component y_{ij} in Eq. (8), is given as $Y = X^\dagger D X$. Because $YY^\dagger = Y^\dagger Y = I$, Y is also unitary.

The Hermitian matrix Z^{MI} can be represented as

$$Z^{\text{MI}} = (Y P_{L/2} Y^\dagger)^T, \quad P_{L/2} = \begin{pmatrix} I_{L/2} & 0_{L/2} \\ 0_{L/2} & 0_{L/2} \end{pmatrix}, \quad (\text{B1})$$

where $I_{L/2}$ and $0_{L/2}$ are, respectively, an $L/2 \times L/2$ identity matrix and an $L/2 \times L/2$ zero matrix. Since $P_{L/2}$ is a projection matrix, satisfying $P_{L/2}^2 = P_{L/2}$, we immediately obtain $(Z^{\text{MI}})^2 = Z^{\text{MI}}$. Therefore, the matrix Z^{MI} is a projection matrix. Note that this argument holds for any Hermitian Hamiltonian H , in particular, containing long-range hopping parameters with randomness.

Appendix C: Quench to finite U from the MI and CDW initial states

As shown in Fig. 4(b), when the system is quenched to the noninteracting point ($U = 0$) starting from the CDW initial state, the Rényi entanglement entropy after the long-time evolution deviates from the Page value. When the system is quenched to finite U , it is expected that thermalization occurs and the Rényi entanglement entropy approaches the Page value after the long-time evolution. These facts indicate that there is a jump between saturated values of the Rényi entanglement entropy for the $U = 0$ and finite U quenches.

To confirm this, we calculate the time evolution of the Rényi entanglement entropy for the quench to finite U starting from the MI and CDW states by the exact diagonalization method [87, 88] and compare it with that for the $U = 0$ quench, as shown in Figs. 7(a,b). In the case of CDW quench [see Fig. 7(b)], we observe the jump between the entanglement entropies of $U = 0$ and small but finite U . We also find that the Rényi entanglement entropies for finite U converge to the Page value. Thus, we can distinguish whether the state is thermalized (for $U > 0$) or not (for $U = 0$) from the Rényi entanglement entropy of the CDW initial states. This is in contrast to the case where the initial state is taken as the MI state because there is no jump (or a very small jump even if it exists) [see Fig. 7(a)].

-
- [1] M. A. Nielsen and I. L. Chuang, *Quantum Computation and Quantum Information* (Cambridge University Press, 2010).
 - [2] C. Holzhey, F. Larsen, and F. Wilczek, *Nucl. Phys. B* **424**, 443 (1994).
 - [3] P. Calabrese and J. Cardy, *J. Stat. Mech.* **2004**, P06002 (2004).
 - [4] P. Calabrese and J. Cardy, *J. Phys. A: Math. Theor.* **42**, 504005 (2009).
 - [5] G. Vidal, J. I. Latorre, E. Rico, and A. Kitaev, *Phys. Rev. Lett.* **90**, 227902 (2003).
 - [6] J. Eisert, M. Cramer, and M. B. Plenio, *Rev. Mod. Phys.* **82**, 277 (2010).
 - [7] N. Laflorencie, *Phys. Rep.* **646**, 1 (2016).
 - [8] A. Kitaev and J. Preskill, *Phys. Rev. Lett.* **96**, 110404 (2006).
 - [9] M. Levin and X.-G. Wen, *Phys. Rev. Lett.* **96**, 110405 (2006).
 - [10] Y. Zhang, T. Grover, and A. Vishwanath, *Phys. Rev. B* **84**, 075128 (2011).
 - [11] S. V. Isakov, M. B. Hastings, and R. G. Melko, *Nat. Phys.* **7**, 772 (2011).
 - [12] K. Życzkowski, *Open Syst. Inf. Dyn.* **10**, 297 (2003).
 - [13] A. J. Daley, H. Pichler, J. Schachenmayer, and P. Zoller, *Phys. Rev. Lett.* **109**, 020505 (2012).
 - [14] D. A. Abanin and E. Demler, *Phys. Rev. Lett.* **109**, 020504 (2012).
 - [15] M. Greiner, O. Mandel, T. Esslinger, T. W. Hänsch, and I. Bloch, *Nature* **415**, 39 (2002).
 - [16] R. Islam, R. Ma, P. M. Preiss, M. Eric Tai, A. Lukin, M. Rispoli, and M. Greiner, *Nature* **528**, 77 (2015).
 - [17] A. M. Kaufman, M. E. Tai, A. Lukin, M. Rispoli, R. Schittko, P. M. Preiss, and M. Greiner, *Science* **353**, 794 (2016).
 - [18] P. Calabrese and J. Cardy, *J. Stat. Mech.* **2005**, P04010 (2005).
 - [19] R. Yoshii, S. Yamashika, and S. Tsuchiya, *J. Phys. Soc. Jpn.* **91**, 054601 (2022).
 - [20] G. D. Chiara, S. Montangero, P. Calabrese, and R. Fazio, *J. Stat. Mech.* **2006**, P03001 (2006).
 - [21] J. H. Bardarson, F. Pollmann, and J. E. Moore, *Phys. Rev. Lett.* **109**, 017202 (2012).
 - [22] A. Bauer, F. Dorfner, and F. Heidrich-Meisner, *Phys. Rev. A* **91**, 053628 (2015).
 - [23] S. Goto and I. Danshita, *Phys. Rev. B* **99**, 054307 (2019).
 - [24] A. M. Läuchli and C. Kollath, *J. Stat. Mech.* **2008**, P05018 (2008).
 - [25] M. Kunimi and I. Danshita, *Phys. Rev. A* **104**, 043322 (2021).
 - [26] C. Rylands, B. Bertini, and P. Calabrese, *arXiv:2206.07985*.
 - [27] V. Alba and P. Calabrese, *Proc. Natl. Acad. Sci. U.S.A.* **114**, 7947 (2017).
 - [28] R. Yao and J. Zakrzewski, *Phys. Rev. B* **102**, 104203 (2020).
 - [29] M. Fagotti and P. Calabrese, *Phys. Rev. A* **78**, 010306 (2008).
 - [30] S. Yamashika, D. Kagamihara, R. Yoshii, and

- S. Tsuchiya, in preparation.
- [31] V. Alba and P. Calabrese, *SciPost Phys.* **4**, 017 (2018).
 - [32] I. Frérot and T. Roscilde, *Phys. Rev. B* **92**, 115129 (2015).
 - [33] M. Cramer, C. M. Dawson, J. Eisert, and T. J. Osborne, *Phys. Rev. Lett.* **100**, 030602 (2008).
 - [34] P. Barmettler, D. Poletti, M. Cheneau, and C. Kollath, *Phys. Rev. A* **85**, 053625 (2012).
 - [35] M. Cheneau, P. Barmettler, D. Poletti, M. Endres, P. Schauß, T. Fukuhara, C. Gross, I. Bloch, C. Kollath, and S. Kuhr, *Nature* **481**, 484 (2012).
 - [36] R. Berkowitz and P. Devlin, *Isr. J. Math.* **224**, 437 (2018).
 - [37] Y. Takasu, T. Yagami, H. Asaka, Y. Fukushima, K. Nagao, S. Goto, I. Danshita, and Y. Takahashi, *Sci. Adv.* **6**, eaba9255 (2020).
 - [38] S. Trotzky, Y.-A. Chen, A. Flesch, I. P. McCulloch, U. Schollwöck, J. Eisert, and I. Bloch, *Nat. Phys.* **8**, 325 (2012).
 - [39] J. Zhang and M. A. Rajabpour, *J. Stat. Mech.* **2021**, 093101 (2021).
 - [40] S.-G. Hwang, *Amer. Math. Mon.* **111**, 157 (2004).
 - [41] S. Fisk, *Amer. Math. Mon.* **112**, 118 (2005).
 - [42] M. Marcus, *Amer. Math. Mon.* **67**, 215 (1960).
 - [43] H. S. Wilf, *Canad. J. Math* **18**, 758 (1966).
 - [44] R. Merris, *Amer. Math. Mon.* **80**, 791 (1973).
 - [45] S. Friedland, *Ann. Math.* **110**, 167 (1979).
 - [46] H. Minc, *Permanents*, *Encyclopedia of Mathematics and Its Applications*, Vol. 6 (Cambridge University Press, 1984).
 - [47] G.-S. Cheon and I. M. Wanless, *Linear algebra and its applications* **403**, 314 (2005).
 - [48] M. Laurent and A. Schrijver, *Amer. Math. Mon.* **117**, 903 (2010).
 - [49] L. Gurvits and A. Samorodnitsky, in *2014 IEEE 55th Annual Symposium on Foundations of Computer Science* (2014) pp. 90–99.
 - [50] M. Marcus and M. Newman, *Ann. Math.* **75**, 47 (1962).
 - [51] L. Gurvits, in *Mathematical Foundations of Computer Science 2005*, edited by J. Jędrzejowicz and A. Szepietowski (Springer Berlin Heidelberg, Berlin, Heidelberg, 2005) pp. 447–458.
 - [52] H. J. Ryser, *Combinatorial mathematics*, Vol. 14 (American Mathematical Soc., 1963).
 - [53] R. A. Brualdi and H. J. Ryser, *Combinatorial matrix theory* (Cambridge University Press, 1991).
 - [54] D. G. Glynn, *Eur. J. Combinat.* **31**, 1887 (2010).
 - [55] K. Balasubramanian, *Combinatorics and diagonals of matrices*, Ph.D. thesis, Indian Statistical Institute-Kolkata (1980).
 - [56] E. Bax and J. Franklin, CalTech-CS-TR-96-04 (1996).
 - [57] E. T. Bax, *Finite-difference algorithms for counting problems* (California Institute of Technology, 1998).
 - [58] D. G. Glynn, *Des. Codes Cryptogr.* **68**, 39 (2013).
 - [59] F. Gray, *United States Patent Number 2632058* (1953).
 - [60] A. Nijenhuis and H. S. Wilf, *Combinatorial algorithms: for computers and calculators* (Elsevier, 1978).
 - [61] B. Gupt, J. Izaac, and N. Quesada, *J. Open Source Software* **4**, 1705 (2019).
 - [62] A. Neville, C. Sparrow, R. Clifford, E. Johnston, P. M. Birchall, A. Montanaro, and A. Laing, *Nat. Phys.* **13**, 1153 (2017).
 - [63] J. Wu, Y. Liu, B. Zhang, X. Jin, Y. Wang, H. Wang, and X. Yang, *Natl. Sci. Rev.* **5**, 715 (2018).
 - [64] P.-H. Lundow and K. Markström, *J. Comput. Phys.* **455**, 110990 (2022).
 - [65] S. Chin and J. Huh, *Sci. Rep.* **8**, 6101 (2018).
 - [66] A. Flesch, M. Cramer, I. P. McCulloch, U. Schollwöck, and J. Eisert, *Phys. Rev. A* **78**, 033608 (2008).
 - [67] M. Cramer, A. Flesch, I. P. McCulloch, U. Schollwöck, and J. Eisert, *Phys. Rev. Lett.* **101**, 063001 (2008).
 - [68] I. Frérot and T. Roscilde, *Phys. Rev. Lett.* **116**, 190401 (2016).
 - [69] G. Biroli, C. Kollath, and A. M. Läuchli, *Phys. Rev. Lett.* **105**, 250401 (2010).
 - [70] S. Sorg, L. Vidmar, L. Pollet, and F. Heidrich-Meisner, *Phys. Rev. A* **90**, 033606 (2014).
 - [71] D. N. Page, *Phys. Rev. Lett.* **71**, 1291 (1993).
 - [72] A. Russomanno, M. Fava, and R. Fazio, *Phys. Rev. B* **102**, 144302 (2020).
 - [73] G. Carleo, F. Becca, L. Sanchez-Palencia, S. Sorella, and M. Fabrizio, *Phys. Rev. A* **89**, 031602 (2014).
 - [74] K. Nagao, M. Kunimi, Y. Takasu, Y. Takahashi, and I. Danshita, *Phys. Rev. A* **99**, 023622 (2019).
 - [75] R. Kaneko and I. Danshita, *Commun. Phys.* **5**, 65 (2022).
 - [76] R. Modak and T. Nag, *Phys. Rev. Research* **2**, 012074 (2020).
 - [77] R. Singh, R. Moessner, and D. Roy, *Phys. Rev. B* **95**, 094205 (2017).
 - [78] S. Aubry and G. André, *Ann. Israel Phys. Soc.* **3**, 18 (1980).
 - [79] T. Devakul and D. A. Huse, *Phys. Rev. B* **96**, 214201 (2017).
 - [80] X. Cao, A. Tilloy, and A. De Luca, *SciPost Phys.* **7**, 024 (2019).
 - [81] O. Alberton, M. Buchhold, and S. Diehl, *Phys. Rev. Lett.* **126**, 170602 (2021).
 - [82] T. Minato, K. Sugimoto, T. Kuwahara, and K. Saito, *Phys. Rev. Lett.* **128**, 010603 (2022).
 - [83] M. Block, Y. Bao, S. Choi, E. Altman, and N. Y. Yao, *Phys. Rev. Lett.* **128**, 010604 (2022).
 - [84] T. Müller, S. Diehl, and M. Buchhold, *Phys. Rev. Lett.* **128**, 010605 (2022).
 - [85] S. Aaronson and A. Arkhipov, in *Proceedings of the forty-third annual ACM symposium on Theory of computing* (2011) pp. 333–342.
 - [86] S. Aaronson and T. Hance, *Quantum Inf. Comput.* **14**, 541 (2014).
 - [87] P. Weinberg and M. Bukov, *SciPost Phys.* **2**, 003 (2017).
 - [88] P. Weinberg and M. Bukov, *SciPost Phys.* **7**, 020 (2019).
 - [89] J.-H. Jung and J. D. Noh, *J. Korean Phys. Soc.* **76**, 670 (2020).
 - [90] J. Schnack, P. Hage, and H.-J. Schmidt, *J. Comput. Phys.* **227**, 4512 (2008).
 - [91] J. Zhang and R. Dong, *Eur. J. Phys.* **31**, 591 (2010).
 - [92] A. Szabados, P. Jeszczyszki, and P. R. Surján, *Chem. Phys.* **401**, 208 (2012).
 - [93] D. Raventós, T. Graß, M. Lewenstein, and B. Juliá-Díaz, *J. Phys. B: At. Mol. Opt. Phys.* **50**, 113001 (2017).